IEEE Access
Multidisciplinary | Rapid Review | Open Access Journal

Received July 16, 2018, accepted August 17, 2018, date of publication August 22, 2018, date of current version September 7, 2018.

Digital Object Identifier 10.1109/ACCESS.2018.2866685

An Efficient p-Trail Based Protection Algorithm With Load Balance in Electric Power Communication Network

BIN LI[1], CHAO LU[1], SIFANG LIU[1], YI SUN[1], BING QI[1], CHAOYANG ZHU[2], DEZHI LI[3], AND SONGSONG CHEN[3]

[1]School of Electrical and Electronic Engineering, North China Electric Power University, Beijing 102206, China
[2]Information and Communication Branch, State Grid Suzhou Power Supply Co. Ltd., Suzhou 215004, China
[3]China Electric Power Research Institute, Beijing 100192, China

Corresponding author: Chao Lu (luchaao@foxmail.com)

This work was supported in part by the National Natural Science Foundation of China under Grant 51777068 and in part by the Science and Technology Projects through State Grid Corporation under Grant SGJSSZ00FZWT1701004.

ABSTRACT Internet of Energy is promoting the deep integration between power grid and communication technologies, while the production, operation and service mode of the power grid are undergoing great evolutions. The expanded services need to be carried by efficient electric power communication network (EPCN). Aiming at releasing the bottleneck problem of link capacity in EPCN, we propose a pre-cross-connected trail (p-Trail)-based protection algorithm with load balance (TPLB) in this paper. First, we introduce the current statue and developing trend of EPCN and analyze traffic flow characteristics of various electric communication services. Then the protecting principles and implementing steps of the proposed TPLB algorithm are described in detail, in which an efficient load balancing algorithm is designed to groom the traffic flow. Finally, the validity and efficiency of TPLB is verified and analyzed in a real EPCN topology from a city of Jiangsu Province, China. It is demonstrated from the simulation results that compared with the existing algorithms, the proposed TPLB can further decrease the network redundancy and blocking probability, and improve the utilization of wavelength resources.

INDEX TERMS p-Trail, electric power communication network, load balance, network survivability, redundancy.

I. INTRODUCTION

As an indispensable platform support of the Internet of energy (IoE) [1], the electric power communication network (EPCN) [2], [3] is essential for realizing the equipment control, information acquisition and demand response of smart grid. With the gradual deployment and advancement of IoE, cloud service, data centers [4], disaster recovery [5] and other large-scale services are in the ascendant, thereby the access objects of EPCN will be more extensive, which requires the EPCN to be capable of providing wider bandwidth and possessing more flexible bandwidth access ability. Meanwhile, the integration between power grid and communication network is deepening, making the grid becomes a so called cyber physical system (CPS) [6], thus a single link or node failure of communication network may lead to cascading failures of power network [7], which puts forward higher requirements for the viability and service recovery ability of EPCN.

Currently, the core and sink nodes of EPCN are mainly backed up by redundant paths or link-disjoint dual routes in China [8]. The current survivability schemes, including classical dedicated path protection methods, i.e., 1+1/1:1 dual routing and self-healing ring [9], [10], are of low resource utilization and lead to high redundancy of the network. However, the new electric services are converging to the upper level backbone network and will occupy more bandwidth resources. It may cause bottlenecked links and bandwidth congestion if EPCN still adopts the traditional protection methods extensively. With the gradual evolution of EPCN from the ring network with poor reliability to the mesh network with high connectivity [11], the novel protection structure will play an important role in saving wavelength resources and decreasing network redundancy.

The preconfigured cycle (p-Cycle) [12] is a fast and efficient protection structure that connects a series of nodes to a simple cycle using backup wavelengths by traversing a node or span at most once. Owing to its pre-cross-connectivity property, the *p*-Cycle could share the pre-configured backup resources and provide fast switching once the link on it fails [13]. However, the *p*-Cycle requires the preconfigured connections of a series of nodes to be a simple cycle, which restricts its application in sparse network and wastes wavelength resources due to its long length. The pre-cross-connected path protection trail [14], short for *p*-Trail, is another preconfigured protection structure that allows the path traversing a node multiple times but a link at most once [15]. Similar to *p*-Cycle, *p*-Trail preforms the fast protection switching speed like *p*-Cycle for the pre-cross-connectivity feature but removes the cycle constraint by allowing arbitrary protection trails, thus it is more flexible than traditional linear protection schemes and *p*-Cycle, and it could derive better capacity efficiency compared with *p*-Cycle [16]. Wu *et al.* [15] design an integer linear programming (ILP) model of non-simple *p*-Cycle and *p*-Trail to obtain the optimal capacity gain in small network. A design model of *p*-Trail was developed using column generation in [16], which could achieve the balance between capacity redundancy and recovery delay. Kiaei *et al.* [17] propose and solve two *p*-Trail configuration problems using models mentioned above. Existing researches of *p*-Trail mainly focus on optimal resource configuration using large solution model with high computing capability requirement and great time overhead, but ignore that the service characteristics of real network, and the exorbitant computation time is unacceptable for real-time and dynamic traffics. In addition, the previous literatures of *p*-Trail were mainly carried out in wavelength division multiplexing (WDM) networks and elastic optical networks (EONs) with high connectivity, the traffic flow is generated randomly, and there is no difference in link capacity in these test network, whose results are of limited reference value for EPCN.

On the other side, some works had carried out to solve the routing and survivability for both unicast and multicast services. Dinh *et al.* [18] propose a novel Arc Removal Light-Hierarchy (ARLH) for the routing of multicast request. Different from light tree, the light hierarchy has no duplicated arc but is free of repetition of nodes, which could decrease the blocking probability. A network with multicast and unicast is modeled in [19] and [20], but the authors does not consider the protection of the two different types of requests jointly. Bejerano and Koppol [21] design a link-coloring based protection scheme for dynamic multicast and unicast connections. The scheme computes two redundant trees (RT) for multicast request, and could accommodate to the addition and removal of single link or node. However, RT-pair is unavailable in some case and the protection cost of which is high. Mehta *et al.* [22] propose control plane based methods for provisioning guaranteed unicast and multicast services respectively, but whose basic idea for multicast protection is still redundant multicast tree. In [23], dynamic provisioning of survivable heterogeneous multicast and unicast traffic are considered jointly, and some heuristic algorithms are proposed for searching RT-pair. However, in its simulation, the proportion between multicast traffic and unicast traffic is assumed to be fixed, i.e. 0.5, which could not verify the performance of the algorithms under various network states. There are both unicast connections and multicast sessions in EPCN, and the quantitative proportion of the two types of services is changeable according to the status of power grid. Thus, a routing and protection algorithm for EPCN should be validated comprehensively.

The focus of this paper is to apply the *p*-Trail to protect multicast and unicast services in EPCN considering the service features and real network conditions. The contributions of our work are summarized as follows.

1) We design an efficient *p*-Trail protection scheme for multicast request whose performances are better than p-Cycle based and redundant tree based algorithms.
2) We propose a novel load balance strategy that considers the node connectivity and can effectively balance the traffic flow in EPCN.
3) We test the serviceability of *p*-Trail under different network states and demonstrate its superiority and robustness over other protection schemes.

As the algorithm proposed in the paper is heuristic, the time of searching a near-optimal *p*-Trail for a request is short. Besides, the network redundancy is decreased by multiplexing the configured *p*-Trails in network, and the blocking probability under different network states with load balance strategy is also decreased compared with the *p*-Cycle based scheme.

The rest of this paper is organized as follows. Section II analyzes the electric services in EPCN. The protection principles of TPLB and load balance strategy are described in section III. Then section IV describes the execution steps of TPLB in detail. In section V, we compare the performance between TPLB and other algorithms by simulation results. Section VI concludes the paper.

II. SERVICES IN EPCN

The modernizing construction of smart grid and Internet of energy puts forward new demand for resource management of EPCN. Meanwhile, the characteristics of electric power communication services also changed greatly [24]–[26]. In general, there are three development trends of the services. Firstly, the traditional power dispatching service and other low bandwidth services will turn from 64 kbit/s and 2 Mbit/s to 1 Gbit/s Ethernet (GE) or even 10 GE. The bandwidth requirement of real-time and management information services will also increase rapidly and concentrate on the dispatching center. Meanwhile, a large amount of data exchange is needed between smart substations in EPCN, and the demand for various kinds of services, such as demand response notification, high definition video, and multi-media, etc., are increasing dramatically. In addition, the new services and applications of smart grid that may be derived in the future will also raise higher requirements of EPCN, such as dynamic load interaction, differentiated quality of service (QoS) supply, etc.

In order to improve the perception and control ability of the smart grid, and support diverse emerging consumer-side and utility-side applications [27], it is necessary to explore the application of novel network protection technologies to enhance the topology survivability and service recoverability of EPCN.

III. BASIC IDEAS OF TPLB

A. *p*-TRAIL BASED PROTECTION PRINCIPLES FOR MULTICAST REQUEST

Multicast request can be denoted as $R = \{s, D\}$, where s is the source node, and $D = \{d_1, d_2, \ldots, d_n\}$ is a set of destination nodes. To resist any single link failure on a multicast tree T, there must be at least two link-disjoint paths between each destination node and source node [28]. In figure 1(a), a multicast request $R_1 = \{1; 4, 6, 9\}$ arrives at network G, and the corresponding routing light tree T_1 is $\{1 \rightarrow 4 \rightarrow 8 \rightarrow 7 \rightarrow 6, 8 \rightarrow 9\}$, as shown by blue lines in figure 1(a).To protect T_1, an approach called pruned Prim's heuristic based link-disjoint tree (PPH-LDT) [29], was proposed to compute another link-disjoint backup tree $T_2\{1 \rightarrow 2 \rightarrow 6, 2 \rightarrow 7, 1 \rightarrow 5 \rightarrow 4, 5 \rightarrow 9\}$ for T_1 in G, as shown by dotted lines in figure 1(b). A *p*-Cycle based protection algorithm for multicast service [30] connects the source node and all destination nodes to a simple cycle to protect single failure of the tree, as shown in figure 1(c), where the corresponding *p*-Cycle is 1-4-8-9-10-6-7-3-1.

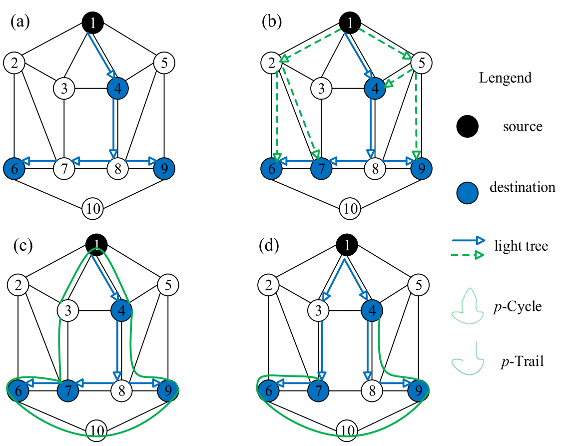

FIGURE 1. Various protection methods for multicast request. (a) The multicast tree; (b) the link-disjoint backup tree; (c) the *p*-Cycle based scheme; (d) the *p*-Trail based scheme.

To achieve this, the most cost-effective way is to guarantee all the destinations and source of a request are on a closed cycle. According to Menger's theorem [31] in graph theory, let x and y be two distinct nodes of a connected graph, if it takes at least k other nodes to separate x and y, i.e., node x and y will not connected after deleting the k nodes and the links connected with them, then x and y can be connected by k link-disjoint paths in G. If a graph meets this condition, it is called k-connected graph. Obviously, a cycle is the simplest 2-connected structure.

In the problem of multicast protection, for all destinations and source of a request, connecting all the destinations and source of a multicast request to a cycle could resist any single link failure on the light tree. Specially, if we optimize the multicast tree with two link-disjoint paths originating from the source node, it is only need to connect all the nodes in D to a trail, which is the most efficient protecting method for dynamic traffics.

We found that *p*-Trail shows great advantages in protecting multicast trees. We first optimize the multicast tree T_1 in figure 1(a) to $T_3\{1 \rightarrow 3 \rightarrow 7 \rightarrow 6, 1 \rightarrow 4 \rightarrow 8 \rightarrow 9\}$ in figure 1(d). On T_3, there are two link-disjoined paths, i.e., $1 \rightarrow 3 \rightarrow 7$ and $1 \rightarrow 4$, originating from the source node 1 to the set of destination nodes. Then we connect all the destination nodes of R_1 to a *p*-Trail 4-8-9-10-6-7, which is capable of protecting single failure on T_3. For instance, if node 3 fails, the destination nodes 6 and 7 will lose the multicast signal. Once the failure occurs, the multicast signal could be transmitted through the backup optical path $1 \rightarrow 4 \rightarrow 8 \rightarrow 9 \rightarrow 10 \rightarrow 6 \rightarrow 7$. It is noteworthy that $1 \rightarrow 4$ is a part of the tree which is not affected by the node failure, and the remaining part is a part of *p*-Trail. Similarly, if link 4-8 fails, the destination node 9 will not be able to receive multicast signals, but it can be resumed by $1 \rightarrow 3 \rightarrow 7 \rightarrow 6 \rightarrow 10 \rightarrow 9$. We use redundancy, which is defined as the ratio of the number of backup wavelengths to the number of working wavelengths, to evaluate the protection efficiency of the three methods. As the redundancy of link-disjoint backup tree, *p*-Cycle and *p*-Trail in this case are $6/5 = 120\%$, $8/5 = 160\%$, $5/6 = 83.3\%$, respectively, it is obvious that the *p*-Trail based scheme shows great advantage over the others.

Since unicast service can be regarded as a multicast service with the number of destination nodes equaling to 1, the *p*-Trail only needs to connect the source node and the destination node of the unicast service to form the optical path, and in this case the *p*-Trail degenerates into traditional dual routing protection.

B. *p*-TRAIL REUSE CONDITION

The condition that a *p*-Trail can protect multiple unicast or multicast requests at the same time is that the protected working paths are link-disjoint mutually, as shown in figure 2.

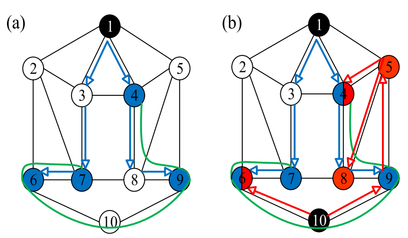

FIGURE 2. Reusing condition of *p*-Trail. (a) A *p*-Trail protects a multicast tree; (b) a *p*-Trail protects two multicast tree.

In figure 2(a), a multicast tree T_1 $\{1 \rightarrow 3 \rightarrow 7 \rightarrow 6, 1 \rightarrow 4 \rightarrow 8 \rightarrow 9\}$ is protected by *p*-Trail 4-8-9-10-6-7.

When another multicast request $R_2 = \{10; 4, 5, 6, 8\}$ arrives at network, we first get a copy G' of the current graph G, then delete the links of T_1 from G', and finally try to construct a multicast tree T_2 for R_2 in G'. If such T_2 is constructed successfully and there are enough free capacity on the links of T_2 in G, the wavelengths on T_2 will be assigned. In the illustration, the acceptable T_2, i.e. $\{10 \rightarrow 6, 10 \rightarrow 9 \rightarrow 5 \rightarrow 4, 5 \rightarrow 8\}$, is constructed successfully, thus the *p*-Trail can protect two multicast requests simultaneously.

C. LOAD BALANCING STRATEGY

At present, the provincial and municipal EPCNs in China encounter the lack of the available optical wavelength in some area, for its explosive growth trend in interaction service between the power grid and the demand side. It is necessary and urgent to groom the traffic and balance the flow's distribution in EPCN so as to make full use of the communication resources and decrease request blocking probability. In addition, the more unified the traffic flow in EPCN is, the larger the network throughput will be. Therefore, the network survivability and network traffic grooming should be considered and achieved together. To balance the whole traffic load, improve the utilization of shared backup resources and reduce bandwidth blocking probability, the routing weight function considering link capacity and node connectivity is designed to groom the traffic flow.

For the services with high quality of protection (QoP) [32] requirement or the services which requires relatively fixed transmission routings, protection relay for instance, the routing paths cannot be balanced, otherwise the working path and backup path will become longer, and the transmission delay and bit error rate will be increased, even leading to the mis-operation of the devices. For this case, we use the k shortest path (KSP) algorithm to search the shortest path of the request, then check whether there is any free capacity on the k^{th} path in an ascending order of hops. If the i^{th} path is available ($1 \leq i < k$), it is not necessary to continue checking, and directly use the path to transport the service; if the k^{th} path is not available, then block the request.

For the services with low QoP requirements, inspired by [33], we can dynamically adjust the routing weights of each link in the network to realize link load balance, so that the traffic flow will be distributed in the network as uniformly as possible. When we use the shortest path algorithm to search route for service request, the more free capacity of the link and the smaller the occupied capacity are, the smaller the weight of the link should be, and the probability of the link being selected as a part of the route link will increase. If a link is selected as a part of the routing path, the two nodes of the link will also process and transmit signals, so the connectivity of the nodes should be considered. The traffic connectivity degree ρ_x of node x is defined as follows.

$$\rho_x = \sum\nolimits_{y \in X} f_{x,y} \Big/ \sum\nolimits_{y \in X} C_{x,y} \tag{1}$$

Where X is a set of nodes adjacent to x, $f_{x,y}$ and $C_{x,y}$ are the free capacity and total capacity on the link x-y under current network state, respectively.

The greater the node connectivity, the smaller the link weight, thus we define the weight function of link x-y as

$$L_{x,y} = \frac{(C_{x,y} - f_{x,y}) \cdot L^0_{x,y}}{f_{x,y} \cdot \rho_x \cdot \rho_y} \tag{2}$$

Where $L_{x,y}$ is the weight of link x-y, $L^0_{x,y}$ is the initial weight determined by the length of the optical cable and routing cost, ρ_x and ρ_y are the traffic connectivity degree of nodes x and y respectively.

To understand this load balance strategy easily, here we illustrate a simple sample in figure 3.

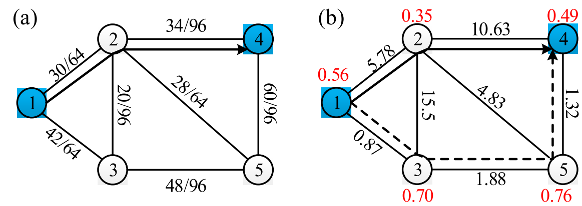

FIGURE 3. Graphic sample of load balance strategy. (a) The traffic distribution in a network; (b) the link weights and node traffic connectivity degree.

Figure 3(a) depicts the capacity of each link in a network at a certain time. For the label on each link, the former represents free capacity, and the latter represents the total capacity of the link. For instance, the total capacity of link 1-2 is 64, and the free capacity is 30. Under this network state, if we search the shortest path for the request node 1 to node 4 as its working path (WP), then WP will be $1 \rightarrow 2 \rightarrow 4$. However, it is observed that the free capacity on links 1-2 and 2-4 is less than links 1-3 and 3-5, respectively. Obviously, choosing path $1 \rightarrow 2 \rightarrow 4$ makes the link 2-4 overload and the bottleneck of node 2 become more serious.

According to (1) and (2), by setting the initial link weight $L^0_{x,y}$ of the link in (2) to 1, we can obtain the traffic connectivity degree of each node and the weight of each link labeling in figure 3(b), where the node connectivity is marked on the node and the link weight is marked around the link. As a comparison, if we search the route for request 1 to 4, the working path will be $1 \rightarrow 3 \rightarrow 5 \rightarrow 4$, which shuns the overloaded link 2-4 and node 2. Hence, the proposed load balance strategy can improve the network throughput by diverting services into a path composed of links with more free capacity and nodes with high connectivity.

IV. ALGORITHM DESCRIPTION

A. THE MAIN STEPS OF TPLB

The flow chart of the proposed TPLB algorithm is illustrated as figure 4. To be specific, the basic steps of TPLB algorithm are described as follows.

Step 1 Input network topology $G = (V, E)$, set simulation parameters.

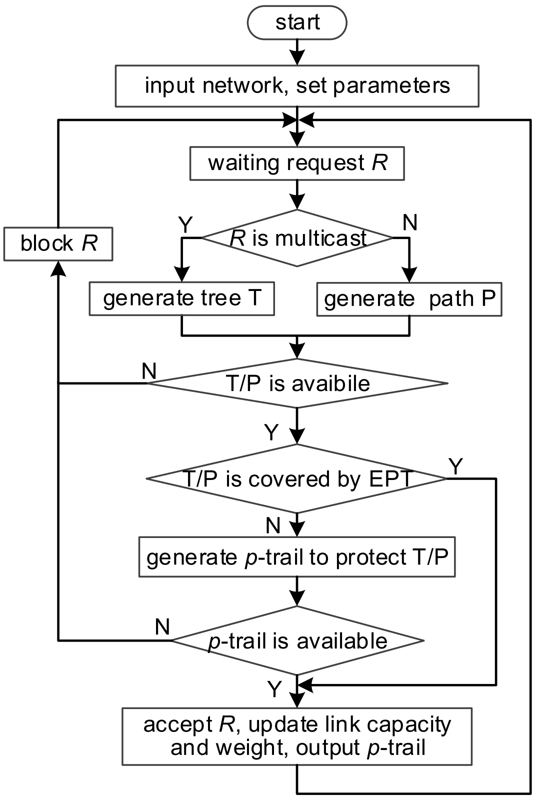

FIGURE 4. **Flow chart of TPLB.**

Algorithm 1 p-Trail Generation Algorithm

Input: $G = (V, E)$, $D = \{d_1, d_{2,\ldots,} d_N\}$

Output: the shortest p-Trail covering all nodes in D

1. **for** $i = 1$: N
2. $D_i = D - d_i$, $G_i = G$
3. **for** each $d_j \in D_i$
4. search the shortest paths from d_i to d_j in G_i
5. **end for**
6. select the shortest path P_{ij} among the paths
7. $D_i = D_i - d_j$, $G_i = G_i - P_{ij}$
8. **while** $D_i \neq \emptyset$
9. **for** each $d \in D_i$
10. search shortest paths from d_i to d and d_j to d in G_i respectively
11. **end for**
12. select two shortest paths P_{im} and P_{jn} respectively
13. **if** $length(P_{im}) < length\ (P_{jn})$
14. Merge P_{im} and P_{ij} into P_{mj}, $D_i{=}D_i - d_m$, $G_i{=}G_i - P_{im}$, $d_i{=}d_m$
15. **else** Merge P_{jn} and P_{ij} into P_{ni}, $D_i{=}D_i - d_n$, $G_i{=}G_i - P_{jn}$, $d_j{=}d_n$
16. **end if**
17. **end while**
18. **end for**
19. **return** the shortest p-Trail generated in **for** loop

Step 2 Wait for the arrival of communication request R.

Step 3 When R arrives, judge whether R is a multicast or unicast request. If R is a multicast request, generate a corresponding light tree (T) using Prim algorithm, otherwise, generate a corresponding light path (P) using Dijkstra algorithm.

Step 4 Judge whether the light tree or path (T/P) is available, i.e., is there enough free capacity on the links of the tree or path. If so, execute Step 5, otherwise, block the request, and turn back to Step 2.

Step 5 Try to search a p-Trail among the existing configured p-Trail (EPT) in the network, which is capable of protecting the tree or path. If such p-Trail exists, then accept the request, update the routing weight of all links, and turn back to Step 2, otherwise execute Step 6.

Step 6 Generate the shortest p-Trail that covers all the destinations of the request.

Step 7 Judge whether the p-Trail is available. If so, output the p-Trail, and update links' routing weight, otherwise, block the request. Turn back to Step 2.

B. *p*-TRAIL GENERATION ALGORITHM

To get a shortest p-Trail that cover all the destinations of a multicast request in Network $G = (V, E)$, we design a heuristic p-Trail generation algorithm, the main idea of which is described in the following pseudocode table.

To understand the algorithm clearly, we give a graphic illustration here. In the sample of figure 5, the nodes to be covered are $D = \{2, 3, 7, 10, 13\}$. If node 3 is selected as the initial node, then lines 3 to 5 calculate the shortest paths from node 3 to node 2, 10, 7, and 13, respectively. Obviously, the shortest path among the paths calculated above is 3-2, thus we delete path 3-2 in G according to lines 6 to 7. Because $D \neq \emptyset$, we continue to calculate the shortest path from 2 to 7, 10, and 13, respectively, and get the shortest path, i.e. path 2-11-10. Similarly, we could obtain the shortest path among the shortest paths from 3 to the left nodes is 3-4-5-13. As the hops of path 2-11-10 is shorter than that of 3-4-5-13, we merge two paths 3-2 and 2-11-10 into a new path 3-2-11-10, as described in lines 9 to 16. Repeating the process, we finally get a trail 3-2-11-10-15-7-6-13 that covers all the given nodes showing in figure 5(d). In the process, we find out that with different initial nodes, the final trails we obtain may be different. To be concrete, if we select node 7 as the initial node, the trail may be a local optimal result. As a result, the whole process is repeated N times with different initial nodes at each time to get the global optimal result.

V. NUMERICAL RESULTS

A. SIMULATION ENVIRONMENT

1) CHARACTERISTICS OF EPCN

In order to test the performance of the proposed algorithm, we select a typical municipal EPCN to run the algorithms. The test network is abstract from a city of Jiangsu province,

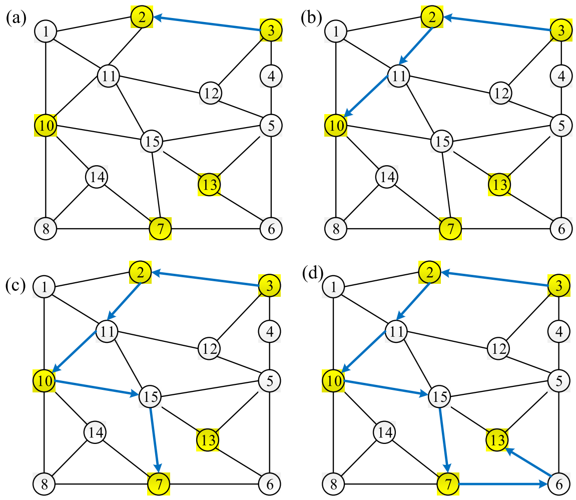

FIGURE 5. Graphic illustration of *p*-Trail generation algorithm.

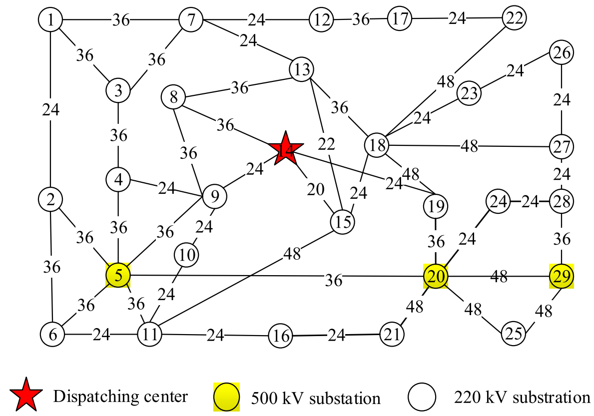

FIGURE 6. An EPCN with 29 nodes and 47 spans (29n47s).

China, including 29 nodes and 47 spans ($29n47s$), with average nodal degree $\overline{d} = 3.24$. The number of available fibers is labeled on each link, and the available wavelength of single core fiber is assumed as 10. In the EPCN, each node has its voltage level and role, which determines its importance and transmission capability of services. Node 14 is a dispatching center of the grid, nodes 5, 20, and 29 are three 500 kV substations, and other nodes are 220 kV substations. It is assumed that all nodes in the network is capable of wavelength conversion and splitting.

2) GENERATION PRINCIPLES OF REQUESTS

We generate both multicast and unicast requests to constitute different network situations to test the serviceability of TPLB. In the simulation, the initial link weight $L^0_{x,y}$ in equation (2) is 1, and the value of k of KSP algorithms used in TPLB is 3. As services in EPCN are mostly hierarchical and centralized, we assume that 80% of the services are launched and transmitted between 220 kV substations and 500 kV substations, and the other 20% are randomly distributed in the network [34]. For centralized sessions, according to the voltage level of substations, the source node of a request is selected among the three 500 kV substations and one dispatching center, and the destination nodes are selected from the adjacent substations which are not more than 3 hops to the according source node [35]. For stochastic request, the source and destinations are randomly selected from the network. In order to verify the effectiveness of the proposed TPLB and its superiority to the existing algorithms, this paper chooses the classic PPH-LDT protection method introduced in figure 1(b), the PBCM algorithm proposed in [30], and the sequential request (seqR) algorithm proposed in [18] as comparisons. Note that we first use the seqR algorithm to search an ARLH as a working routing for a request, then another ARLH, which is link-disjointed with the working routing, is searched as its backup routing. Meanwhile, to verify the effectiveness of the proposed load balancing strategy, we use a dynamic loading balancing (DLB) strategy proposed in [36] as a comparison, the corresponding algorithm is named *p*-Trail based protection algorithm with dynamic load balancing (TP-DLB).

We use two statistical indicators to evaluate the performance of these algorithms.

1) Blocking probability, i.e., the ratio between the number of blocked requests to the number of total launched requests.
2) Network redundancy, i.e., the ratio between the total number of backup wavelengths to the total number of working wavelengths [37], as defined in (3).

$$r = \sum\nolimits_{l \in E} p_l^\lambda \Big/ \sum\nolimits_{l \in E} w_l^\lambda \tag{3}$$

Where l represents the link, E represents the link set of the network, w_l^λ and p_l^λ represents the number of working wavelengths and backup wavelengths on link l, respectively.

Under specific network conditions, the lower the blocking probability and network redundancy are, the better the performance of routing and protection algorithms will be.

B. SIMULATION RESULTS

1) SETTINGS OF SIMULATIONS

To test the performance of the algorithms under different communication pressures and request properties, we design the simulations by setting up three scenarios. Note that, because the simulations are carried out in real EPCN, the total wavelengths on each link is fixed for three scenario.

i) Given unicast proportion α and the number of destinations of a multicast request $|D|$, evaluate the performance of the algorithms versus request number $|R|$. In particular, $\alpha = 0.3$, $|D| = 5$, and $|R|$ varying in the array $(100, 200, \ldots, 2000)$. That is, among the 2000 dynamic requests generated one by one, there are about 1400 multicast requests with 5 destination nodes, the others are unicast requests. Figures 7 to 8 show the blocking probability and redundancy of different algorithms versus request numbers.

ii) Given the number of requests $|R|$ and the number of destinations of a multicast request $|D|$, evaluate the performance of the algorithms versus the multicast proportion a. In particular, $|R| = 800$, $|D| = 5$, and α varies in the array $(0.1, 0.2, \ldots, 0.9)$. Figures 8 and 9 illustrate the blocking probability and redundancy of algorithms versus unicast proportions.

iii) Given the number of destinations of a multicast request $|D|$, evaluate the performance of the algorithms versus the multicast proportion and request number $|R|$. In particular, $|D| = 5$, a varies in the array $(0.1, 0.2, \ldots, 0.9)$, and $|R|$ varies in the array $(100, 200, \ldots, 1000)$. Because the performance of the algorithm is associated with two variables, the simulation results are provided in the form of 3D in figures 11 and 12.

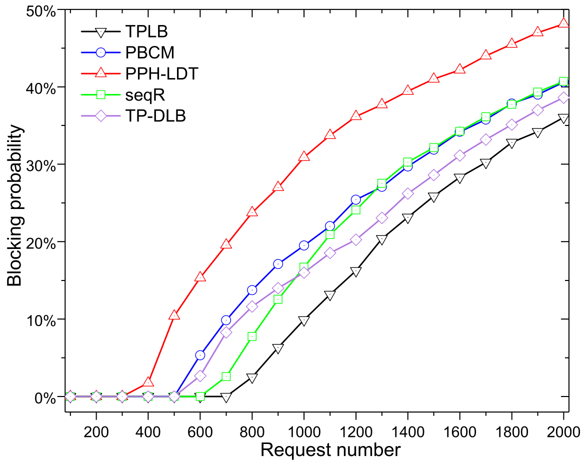

FIGURE 7. Blocking probability of different algorithms versus request numbers with $\alpha = 0.3$.

2) PERFORMANCE OF THE ALGORITHMS VERSUS REQUEST NUMBER

Figure 7 provides the values obtained for the blocking probability versus request number in the EPCN. As expected, all blocking probability values are increasing with the request numbers. Here we observe a significant improvement of TPLB over PBCM, seqR and traditional PPH-LDT. To be specific, PPH-LDT, PBCM and seqR begin to block request when request numbers are greater than 400, 500, and 600, respectively. After that, the blocking probability of PPH-LDT keeps the highest level, and the blocking probability gap between PBCM and seqR is narrowing with the increase of request number. Our TPLB scheme does not block request until request number exceeds 750, and its blocking probability is the minimum among the five algorithms when the number of requests are equal. After the algorithms start blocking service, the blocking probability of TPLB is averagely 4.3% lower than that of TP-DLB, 11.7% lower than that of PBCM and 20.8% lower than that of PPH-LDT under the same request numbers. This is due to that PPH-LDT may not be able to search for a backup multicast tree which is link-disjoint with the created working multicast tree under some network states, and the backup multicast tree takes up more wavelength resources than *p*-Cycle and*p*-Trail; On the other hand, the *p*-Trail used by TPLB is shorter than *p*-Cycle in general, and with a flexible and excellent load balancing algorithm, its blocking rate is the lowest.

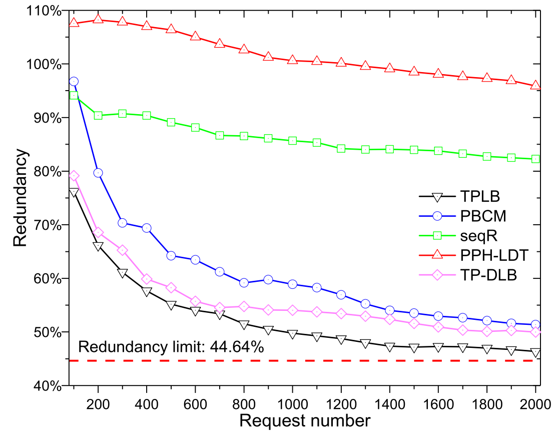

FIGURE 8. Network redundancy of different algorithms versus request numbers with $\alpha = 0.3$.

Figure 8 shows the redundancy comparison of the algorithms with unicast proportion of 0.3. Redundancy represents the ratio of the backup wavelength resource to the working wavelength resource in the network, and the lower the redundancy, the higher the utilization of the backup resource. As the graph shows, with the increase of request number in the network, the redundancy of each algorithm decreases gradually, and the redundancy of PPH-LDT is the highest under the same request number, seqR and PBCM take the second and third place, respectively, and TPLB is the lowest. The average redundancy of PPH-LDT is 105%, whose descending trend is not obvious. Because seqR uses ARLH, which enables the repetition of nodes in the light paths, to route and protect a multicast session, which saves some wavelength resource and therefore derives lower redundancy than PPH-LDT. The redundancy of seqR and PBCM are 15% and 36% lower than that of PPH-LDT on average. When the request number is less than 600, the redundancy of TPLB performs a significant decrease with the increase of request number. After request number is over 700, the redundancy of which is stable to 48.2%, and is 14.3% lower than that of PBCM on average. In addition, when the request number is less than 500, the redundancy of TPLB and TP-DLB are close to each other; while the average redundancy gap between TPLB and TP-DLB is 4.6% after the request number exceeds 800.

Li *et al.* [38] deduced the bound of logical redundancy under m link failures in link-restorable network.

$$r \geq m/\left(\bar{d} - m\right) \tag{4}$$

Where m is the number of link failures that can be protected, and $\overline{d}$ is the average node degree of the network.

For the test network, $\overline{d} = 3.24$, so the minimum value of redundancy under single link failure is 44.64%, as shown in the dotted line in the figure. With the increase of request number, the redundancy of TPLB is getting close to the theoretical limit. This is because that more request means denser traffic, which is beneficial for TPLB to exploit its advantages in saving backup resources. When the request number is more than 1500, the average redundancy gap between TPLB and the theoretical limit is 2.32%, which is very close to the theoretical limit.

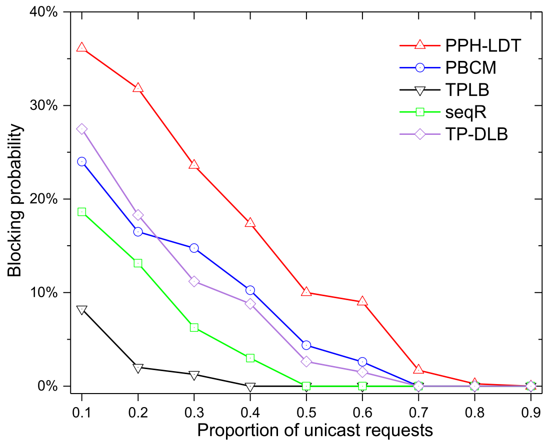

FIGURE 9. Blocking probability of different algorithms versus unicast proportion with $|R| = 800$.

3) PERFORMANCE OF THE ALGORITHMS VERSUS REQUEST PROPORTION

Figure 9 reveals the trend of blocking probability of algorithms with different unicast proportions. It can be seen from the graph that with the increase of unicast service proportion, the blocking probability of each algorithm decreases gradually. When the proportion of unicast service is the same, the blocking rate of PPH-LDT is the highest, PBCM and seqR take the second and third place, respectively, and TPLB is the smallest, which is consistent with the result in figure 7. This is because when the request number is fixed, the more unicast requests, the less the number of wavelength channels will be occupied, and the blocking rate will decrease. In addition, the smaller the proportion of unicast requests, the wider the gap between TPLB and TP-DLB is, which indicates that TPLB shows obvious advantage over TP-DLB under various network states, especially when the traffic is dense. Moreover, we observe that when the unicast proportion exceeds 0.4, the blocking rate of TPLB is 0, while seqR, PBCM and PPH-LDT start to accept any requests when the unicast proportion exceeds 0.5, 0.7 and 0.8, respectively, which fully demonstrates that TPLB can adapt to the changes of the network environment well and provide efficient protection routing for the service even if the proportion of unicast and multicast services is fluctuant. In general, when the proportion of unicast requests is less than 0.5, for the proposed TPLB, the average gaps on blocking probability are 24.3%,

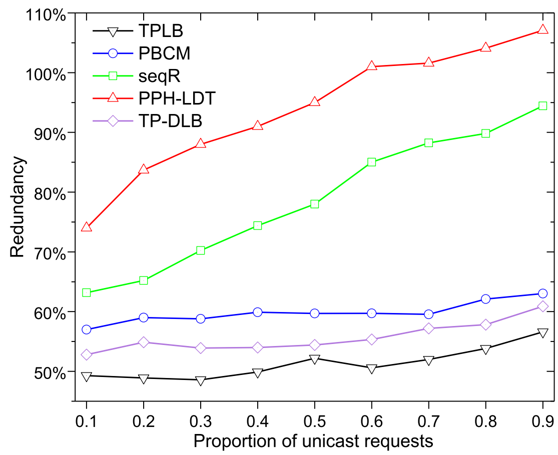

FIGURE 10. Network redundancy of different algorithms versus unicast proportion with $|R| = 800$.

13.5% and 8.8% compared with and PPH-LDT, PBCM and seqR, respectively.

Figure 10 describes the variation of redundancy of different algorithms versus unicast proportion when the request number fixes at 800. With the increase of unicast proportion, the redundancy of PPH-LDT and seqR increase a lot, while there is a minor fluctuation of the redundancy of TPLB and PBCM. This is because the backup trees and backup ARLHs generated by PPH-LDT and seqR are less possible to provide backup paths for other subsequent working requests, so the reusing rate of backup resources in the network is not as high as TPLB does. Therefore, when the unicast proportion is large, the protection schemes of PPH-LDT and seqR are similar to dedicated path protection without sharing of backup resources. On the contrary, p-Trail and p-Cycle generated by TPLB and PBCM respectively for working multicast trees can provide backup paths for newly arrived services, but because p-Trail is statistically shorter than p-Cycle, and the load balancing strategy makes it more effective in selecting links with more free capacity, the redundancy of TPLB is lower than that of PBCM. The redundancy of TP-DLB is between that of TPLB and PBCM, which is 4.3% higher than the former and 4.2% lower than the latter. Overall, the redundancy of TPLB is the lowest, with an average value of 51.3%, while the redundancy of PBCM, seqR and PPH-LDT are 8.5%, 27.4% and 42.6% higher than that of TPLB, respectively.

4) PERFORMANCE OF THE ALGORITHMS VERSUS REQUEST NUMBER AND PROPORTION

To explore the performance of the proposed algorithms under dynamic network situations, we test and analyze network redundancy of TPLB algorithm with diverse request number and unicast proportion, as shown in figure 11. It is clear to conclude that when the unicast proportion is fixed, redundancy decreases with the increase of request number, which is consistent with the results of figure 8, and when the number of

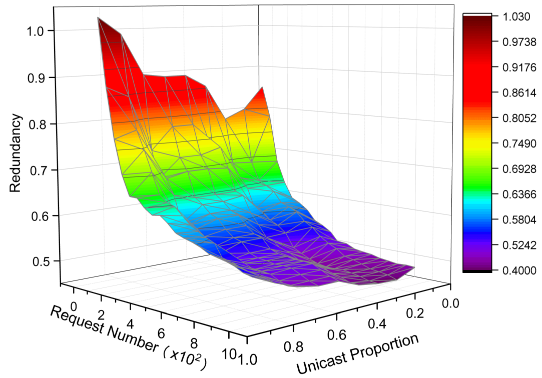

FIGURE 11. Network redundancy of TPLB algorithm versus unicast proportion and request number.

requests is fixed, the redundancy increases with the increase of unicast request ratio, which is consistent with the result of figure 10.

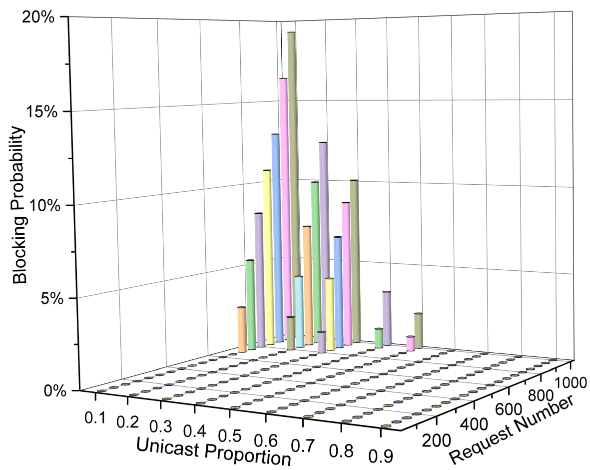

FIGURE 12. Blocking probability of TPLB algorithm versus unicast proportion and request number.

The 3D bar graph, i.e. figure 12, reflects the changing trend of the blocking probability of TPLB versus request number and unicast proportion. As the unicast proportion increases, the overall blocking probability of the network decreases gradually, and the larger the proportion of unicast services, the greater the number of corresponding request number. Since the wavelength resources occupied by unicast services are usually less than multicast services, the consumption rate of free resources in the network is reduced. On the other hand, when the service proportion is constant, the blocking rate increases with the increase of the number of service requests, which is consistent with the result of figure 7.

VI. CONCLUSION

In this paper, we proposed an efficient p-Trail based protection algorithm with load balance (TPLB) and verified its performance in a real EPCN. The application of flexible p-Trail structure in TPLB makes it more excellent in resource utilization than previous redundant tree based and p-Cycle based algorithms, while compared with existing dynamic load balance scheme, the blocking probability of TPLB with the novel load balance strategy is decreased dramatically. Simulation results show that the blocking probability of TPLB is lower than that of PBCM, seqR and PPH-LDT under the same request numbers, respectively. Besides, the redundancy of TPLB is 8.5%, 27.4% and 42.6% lower than PBCM, seqR and PPH-LDT, respectively. We also tested the serviceability of our work under different network states and demonstrated its superiority and robustness.

REFERENCES

[1] M. H. Y. Moghaddam and A. Leon-Garcia, "A fog-based Internet of energy architecture for transactive energy management systems," *IEEE Internet Things J.*, vol. 5, no. 2, pp. 1055–1069, Apr. 2018, doi: 10.1109/JIOT.2018.2805899.

[2] Q. Wang, M. Pipattanasomporn, M. Kuzlu, Y. Tang, Y. Li, and S. Rahman, "Framework for vulnerability assessment of communication systems for electric power grids," *IET Gener., Transmiss. Distrib.*, vol. 10, no. 2, pp. 477–486, Feb. 2016, doi: 10.1049/iet-gtd.2015.0857.

[3] B. Qi *et al.*, "An emerging survivability technology for dispatching service of electric power communication network," *IEEE Access*, vol. 6, pp. 21231–21241, May 2018, doi: 10.1109/ACCESS.2018.2823745.

[4] D. Wang, "Basic framework and key technology for a new generation of data center in electric power corporation based on cloud computation," *Automat. Electr. Power Syst.*, vol. 36, no. 11, pp. 1066–1067, Jun. 2012, doi: 10.3969/j.issn.1000-1026.2012.11.012.

[5] J. Liu, C. H. Xia, N. B. Shroff, and H. D. Sherali, "Distributed optimal load shedding for disaster recovery in smart electric power grids: A second-order approach," *ACM SIGMETRICS Perform. Eval. Rev.*, vol. 42, no. 1, pp. 591–592, Jun. 2014, doi: 10.1145/2637364.2592036.

[6] M. H. Cintuglu, O. A. Mohammed, K. Akkaya, and A. S. Uluagac, "A survey on smart grid cyber-physical system testbeds," *IEEE Commun. Surveys Tuts.*, vol. 19, no. 1, pp. 446–464, 1st Quart., 2017, doi: 10.1109/COMST.2016.2627399.

[7] Y. Cai, Y. Cao, Y. Li, T. Huang, and B. Zhou, "Cascading failure analysis considering interaction between power grids and communication networks," *IEEE Trans. Smart Grid*, vol. 7, no. 1, pp. 530–538, Jan. 2016, doi: 10.1109/TSG.2015.2478888.

[8] B. Li, B. Qi, Y. Sun, H. Yan, and S. Chen, "Applications of forecasting based dynamic p-cycle reconfiguration under reliable optical network in smart grid," *Comput. Commun.*, vol. 49, no. 8, pp. 48–59, Aug. 2014, doi: 10.1016/j.comcom.2014.05.002.

[9] D. Griffith and S. Lee, "A 1+1 protection architecture for optical burst switched networks," *IEEE J. Sel. Areas Commun.*, vol. 21, no. 9, pp. 1384–1398, Nov. 2003, doi: 10.1109/JSAC.2003.818231.

[10] X. Sun, C. K. Chan, Z. Wang, C. Lin, and L. K. Chen, "A single-fiber bi-directional WDM self-healing ring network with bi-directional OADM for metro-access applications," *IEEE J. Sel. Areas Commun.*, vol. 25, no. 3, pp. 18–24, Apr. 2007, doi: 10.1109/JSAC-OCN.2007.023305.

[11] X. Jin *et al.*, "Research and prospect of survivability technology in power optical transmission network," *Electr. Power Inform. Commun. Technol.*, vol. 12, no. 10, pp. 69–72, Oct. 2014.

[12] R. Asthana, Y. N. Singh, and W. D. Grover, "P-cycles: An overview," *IEEE Commun. Surveys Tuts.*, vol. 12, no. 1, pp. 97–111, 1st Quart., 2010, doi: 10.1109/SURV.2010.020110.00066.

[13] A. Metnani and B. Jaumard, "Stability of FIPP *p*-cycles under dynamic traffic in WDM networks," *IEEE/ACM Trans. Netw*, vol. 21, no. 2, pp. 413–425, Apr. 2013, doi: 10.1109/TNET.2012.2200905.

[14] T. Y. Chow, F. Chudak, and A. M. Ffrench, "Fast optical layer mesh protection using pre-cross-connected trails," *IEEE/ACM Trans. Netw.*, vol. 12, no. 3, pp. 539–548, Jun. 2004, doi: 10.1109/TNET.2004.828951.

[15] B. Wu, K. L. Yeung, and P.-H. Ho, "ILP formulations for non-simple *p*-cycle and p-trail design in WDM mesh networks," *Comput. Commun.*, vol. 54, no. 5, pp. 716–725, Apr. 2010, doi: 10.1016/j.comnet.2009.09.019.

[16] H. Alazemi, S. Sebbah, and M. Nurujjaman, "Fast and efficient network protection method using path pre-cross-connected trails," *J. Opt. Commun. Netw.*, vol. 5, no. 12, pp. 1343–1352, Dec. 2013, doi: 10.1364/JOCN.5.001343.

[17] M. S. Kiaei, S. Sebbahm, A. Cerny, H. Alazemi, and C. Assi, "Efficient network protection design models using pre-cross-connected trails," *IEEE Trans. Commun.*, vol. 59, no. 11, pp. 3102–3110, Nov. 2011, doi: 10.1364/JOCN.5.001343.

[18] D. D. Le, F. Zhou, and M. Molnár, "Minimizing blocking probability for the multicast routing and wavelength assignment problem in WDM networks: Exact solutions and heuristic algorithms," *J. Opt. Commun. Netw.*, vol. 7, no. 1, pp. 36–48, Jan. 2015, doi: 10.1364/JOCN.7.000036.

[19] F. Zhang and W.-D. Zhong, "Performance evaluation of optical multicast protection approaches for combined node and link failure recovery," *J. Lightw. Technol.*, vol. 27, no. 18, pp. 4017–4025, Sep. 15, 2009, doi: 10.1109/JLT.2009.2021581.

[20] W.-D. Zhong and F. Zhang, "An overview of *p*-cycle based optical multicast protection approaches in mesh WDM networks," *Opt. Switching Netw.*, vol. 8, no. 4, pp. 259–274, Dec. 2011, doi: 10.1016/j.osn.2011.06.003.

[21] Y. Bejerano and P. V. Koppol, "Link-coloring based scheme for multicast and unicast protection," in *Proc. IEEE Int. Conf. High Perform. Switching Routing*, Taipei, Taiwan, Jul. 2013, pp. 21–28, doi: 10.1109/HPSR.2013.6602285.

[22] S. Mehta, S. Joshi, T. Das, and A. Gumaste, "On control plane algorithms for carrier EtherNet networks: Unicast, multicast provisioning and control traffic reduction," *Opt. Switching Netw.*, vol. 23, no. 1, pp. 52–66, Jan. 2017, doi: 10.1016/j.osn.2016.09.001.

[23] A. Khalil, A. Hadjiantonis, G. Ellinas, and M. Ali, "Dynamic provisioning of survivable heterogeneous multicast and unicast traffic in WDM networks," in *Proc. IEEE Int. Conf. Commun. (ICC)*, Istanbul, Turkey, Jun. 2006, pp. 2465–2470, doi: 10.1109/ICC.2006.255149.

[24] R. H. Khan and J. Y. Khan, "A comprehensive review of the application characteristics and traffic requirements of a smart grid communications network," *Comput. Netw.*, vol. 57, no. 3, pp. 825–845, 2013, doi: 10.1016/j.comnet.2012.11.002.

[25] B. Li, J. Yang, B. Qi, Y. Sun, H. Yan, and S. Chen, "Application of *p*-cycle protection for the substation communication network under SRLG constraints," *IEEE Trans. Power Del.*, vol. 29, no. 6, pp. 2510–2518, Dec. 2014, doi: 10.1109/TPWRD.2014.2358571.

[26] T. Yang, R. Zhao, W. Zhang, and Q. Yang, "On the modeling and analysis of communication traffic in intelligent electric power substations," *IEEE Trans. Power Del.*, vol. 32, no. 3, pp. 1329–1338, Jun. 2017, doi: 10.1109/TPWRD.2016.2573320.

[27] D. A. Chekired, L. Khoukhi, and H. T. Mouftah, "Decentralized cloud-SDN architecture in smart grid: A dynamic pricing model," *IEEE Trans. Ind. Informat.*, vol. 14, no. 3, pp. 1220–1231, Mar. 2018, doi: 10.1109/TII.2017.2742147.

[28] J. Zhang, J. Zhang, Y. Zhao, and W. Gu, "k-regular and k-(edge)-connected protection structures in optical transport networks," in *Proc. IEEE Opt. Fiber Commun. Conf. (OFC)*, Anaheim, CA, USA, Mar. 2013, pp. 1–3.

[29] N. K. Singhal, L. H. Sahasrabuddhe, and B. Mukherjee, "Provisioning of survivable multicast sessions against single link failures in optical WDM mesh networks," *J. Lightw. Technol.*, vol. 21, no. 11, pp. 2587–2594, Nov. 2003, doi: 10.1109/JLT.2003.819550.

[30] L. Bin *et al.*, "P-cycle based protection scheme with cycle multiplexing and capacity balance for multicast service in substation communication network," *Int. J. Electr. Power Energ. Syst.*, vol. 102, pp. 340–348, Nov. 2018, doi: 10.1016/j.ijepes.2018.04.038.

[31] W. T. Tutte, "Menger's theorem for matroids," *J. Res. Nat. Bur. Standards-B, Math. Math. Phys*, vol. 69B, no. 1, pp. 49–53, Jan./Jun. 1965.

[32] S. Samir and J. Brigitte, "Differentiated quality-of-protection in survivable WDM mesh networks using *p*-structures," *Comput. Commun.*, vol. 36, pp. 621–629, Mar. 2013, doi: 10.1016/j.comcom.2012.09.003.

[33] C. K. Constantinou and G. Ellinas, "A load balancing technique for efficient survivable multicasting in mesh optical networks," *Opt. Switching Netw.*, vol. 22, pp. 1–8, Nov. 2016, doi: 10.1016/j.osn.2016.03.002.

[34] X. Liu, T. Hai, J. Zheng, H. Zhu, and D. Xu, "Hot-standby communication of VLAN-based smart substation," *Electr. Power Automat. Equ.*, vol. 35, no. 7, pp. 132–139, Jul. 2015, doi: 10.16081/j.issn.1006-6047.2015.07.021.

[35] B. Li *et al.*, "P-cycle protection algorithm oriented to demand response service," *Automat. Electr. Power Syst.*, vol. 41, no. 23, pp. 8–14, Dec. 2017, doi: 10.7500/AEPS20170610001.

[36] B. Chen *et al.*, "Multi-link failure restoration with dynamic load balancing in spectrum-elastic optical path networks," *Opt. Fiber Technol.*, vol. 18, no. 1, pp. 21–28, 2012, doi: 10.1016/j.yofte.2011.10.002.

[37] M. S. Kiaei, C. Assi, and B. Jaumard, "A survey on the p-cycle protection method," *IEEE Commun. Surveys Tuts.*, vol. 11, no. 3, pp. 53–70, 3rd Quart., 2009, doi: 10.1109/SURV.2009.090305.

[38] X. Li, S. Huang, J. Zhang, Y. Zhao, W. Gu, and Y. Wang, "Analysis and modeling of k-regular and k-connected protection structure in ultra-high capacity optical networks," *China Commun.*, vol. 12, no. 3, pp. 106–119, Mar. 2015, doi: 10.1109/CC.2015.7084369.

BIN LI was born in Beijing, China, in 1983. He received the B.S. and Ph.D. degrees from the State Key Laboratory of Information Photonic and Optical Communications (IPOC), Beijing University of Posts and Telecommunications (BUPT), in 2005 and 2010, respectively. He was a Joint Training Doctor with Yuan Ze University, Taiwan, who focused on the antenna design, antenna measurement, electromagnetic scattering, and asymptotic high frequency techniques.

After graduated from IPOC, BUPT, he was with the Wireless and Optical Networking Research Group, Bell Labs Research, China. He joined North China Electric Power University in 2011, where he is currently an Associate Professor with the Communication Technology Research Center, School of Electric and Electronic Engineering. His research interests include hybrid optical and wireless communication networks, next-generation Internet, electric power communication, network routing, and signaling technology.

He has published over 90 journals and conference papers, and submitted over 20 patents. He is a member of the China Communications Standards Association and the Chinese Society for Electrical Engineering. He has received the certifications from the IBM Rational University Program and always working as an OPNET Training Engineer.

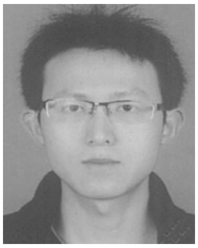

CHAO LU was born in Hanzhong, Shaanxi, China, in 1994. He received the B.S. degree in communication engineering from North China Electric Power University (NCEPU), Beijing, China, in 2016.

He is currently pursuing the master's degree in information and communication technology with NCEPU. He has published five journal papers. His research interests include network survivability and energy Internet. He received the national scholarship in 2017.

SIFANG LIU was born in Changchun, Jilin, China, in 1995. She received the B.S. degree in communication engineering from North China Electric Power University, Beijing, China, in 2017, where she is currently pursuing the master's degree in information and communication engineering.

Her research includes the demand response of power systems and communication of electric power systems. She received the Outstanding Graduates Award from the Beijing Municipal Commission of Education in 2017.

YI SUN was born in Chaoyang, Liaoning, China, in 1972. He received the M.S. degree in communication and information system and the Ph.D. degree in electric information technology from North China Electric Power University (NCEPU), Beijing, China, in 2009 and 2014, respectively. He is currently a Professor with NCEPU.

In recent years, he has been involved in the National Major Special Project and the Ministry of Industry and Electronic Information Industry Development Fund Project. He has rich experience in electric power information and communication. His research interests include smart power consumption, demand response, and power system communication technology.

BING QI was born in Liaoyang, Liaoning, China, in 1965. He received the B.S. and M.E. degrees from Beijing Jiaotong University, Beijing, China, in 1987 and 1990, respectively. He joined North China Electric Power University (NCEPU) in 1990. He is currently a Professor with NCEPU.

He has hosted and participated over 50 national key programs and other programs. He is a Technical Expert of IEC PC-118 and a Consultant with the China Electric Power Research Institute. He has published over 100 journals and conference papers. His research interests include demand side management of smart grid, electric power system analysis, and electric power communication technology.

CHAOYANG ZHU was born in Suzhou, Jiangsu, China, in 1970. He received the B.S. degree from Southeast University, Nanjing, China, and the M.E. degree from Tongji University, Shanghai, China. He joined State Grid Suzhou Power Supply Co. Ltd., in 1992, where he is currently a Senior Engineer.

He has participated in major projects, such as the construction of Suzhou wide area power communication network based on MPLS/VPN and the construction of 4G TD-LTE power wireless network. He has rich professional experience. He engaged in the construction and management of power enterprise informatization, power communication, and dispatch automation.

DEZHI LI was born in Chengde, Hebei, China, in 1982. He is currently an Engineer with the China Electric Power Research Institute, Beijing, China. His research interests include intelligent power consumption, demand response, and energy efficiency management.

SONGSONG CHEN was born in Dongying, Shandong, China, in 1987. He is currently an Engineer with the China Electric Power Research Institute, Beijing, China. His research interests include power system communication, hybrid wireless and optical network planning, and resource allocation algorithms.